Quaternary Research (2017), **87**, 151–167.

doi:10.1017/qua.2016.9

Quaternary marine terrace chronology, North Canterbury, New Zealand, using amino acid racemization and infrared-stimulated luminescence

David O.S. Oakley[a]*, Darrell S. Kaufman[b], Thomas W. Gardner[c], Donald M. Fisher[a], Rebecca A. VanderLeest[a]

[a]Department of Geosciences, Pennsylvania State University, University Park, PA 16802, United States
[b]School of Earth Sciences & Environmental Sustainability, Northern Arizona University, Flagstaff, AZ 86011, United States
[c]Department of Geosciences, Trinity University, One Trinity Place, San Antonio, TX 78212, United States

(Received March 20, 2016; Accepted November 3, 2016)

Abstract

Extensive marine terraces along the North Canterbury coast of the South Island of New Zealand record uplift in this tectonically active area. Although the terraces have been studied previously, applications of Quaternary geochronological techniques to the region have been limited. We use infrared-stimulated luminescence (IRSL), amino acid racemization (AAR), and radiocarbon to determine ages of terraces at three locations—Glenafric, Motunau Beach, and Haumuri Bluff. We develop an AAR calibration curve for the mollusk species *Tawera spissa* from sites of known age, including the sedimentary sequence of the Whanganui Basin. Bayesian model averaging of the results is used to estimate ages of marine shells from the North Canterbury terraces. By using both IRSL and AAR, we are able to confirm ages using two independent dating methods and to identify one IRSL result that is likely in error. We develop new age estimates for the marine terraces of North Canterbury and propose correlations between sites. This terrace chronology differs significantly from most previous studies, highlighting the importance of numerical dating. The most extensive terraces are from marine isotope stages (MISs) 5a and 5c, with partial reoccupation of one terrace during MIS 3, whereas MIS 5e terraces are notably lacking among those dated.

Keywords: Quaternary geochronology; Marine terraces; New Zealand; Amino acid racemization; Luminescence

INTRODUCTION

Marine terraces, formed during sea-level high stands and subsequently uplifted above sea level, represent the combined imprint of the glacioeustatic sea-level cycle and vertical uplift on coastal geomorphology (Lajoie, 1986; Pedoja et al., 2014). When terraces form along an uplifting coast, they can be correlated with known high stands, provided that the ages of the terraces can be determined. This study focuses on the North Canterbury region of New Zealand, where uplift related to active faulting and folding has produced extensive marine terraces along the coast. These terraces have been the subject of a number of previous studies (Jobberns, 1926, 1928; Jobberns and King, 1933; Carr, 1970; Bull, 1984; Yousif, 1987; Barrell, 1989; Ota et al., 1984, 1996), many of which have proposed possible correlations with sea-level high stands, and estimates of their ages have been used in studies that address rates of deformation (Nicol et al., 1994) and the level of seismic hazard (Barrell and Townsend, 2012). Despite this body of work, the terraces remain poorly dated (Ota et al., 1984, 1996), with little geochronological data to support proposed correlations with sea-level high stands. Previous workers have had few options for dating the terraces; most are too old for radiocarbon dating, and corals suitable for uranium series dating have not been found in New Zealand terraces (Pillans, 1990), despite the success of this technique in terrace studies in other parts of the world (e.g., Muhs et al., 1992). More modern techniques, such as luminescence dating and amino acid racemization (AAR), however, provide the opportunity to date the North Canterbury marine terraces and to test previous age estimates.

In this study, we report the results of infrared-stimulated luminescence (IRSL) and AAR analyses of sediments and shells from marine terraces. We use AAR analyses of shells from deposits of known age, predominantly from the Whanganui Basin of the southern part of the North Island, New Zealand, to calibrate the rate of AAR. This study expands on previous AAR studies in the region by analyzing the extent of AAR in multiple amino acids preserved within the intracrystalline fraction of the shell carbonate, and by using newly

*Corresponding author at: Department of Geosciences, Pennsylvania State University, University Park, PA 16802, United States. E-mail address: doo110@psu.edu (D.O.S. Oakley).

developed Bayesian statistical methods for developing an AAR age equation and calculating age uncertainties. We then apply this AAR age model in combination with IRSL to date marine terraces of unknown age along the coast of North Canterbury, South Island. We demonstrate the value of AAR and IRSL as independent, but complementary methods in establishing a terrace chronology, we provide new ages for the North Canterbury terraces that differ from previous estimates, and we develop an AAR chronology for the species *Tawera spissa* extending back to marine isotope stage (MIS) 17 in the region.

BACKGROUND

AAR calibration sample sites

In order to calibrate the AAR age model, mollusk shells were collected from six previously studied sites, the ages of which are known independently from methods other than AAR. Four of these sites are in the Whanganui Basin (Fig. 1). The late Cenozoic marine sedimentary sequence that accumulated in near-shore Whanganui Basin was uplifted (Kamp et al., 2004) and exposed along the coast. Bowen et al. (1998) previously developed an aminostratigraphy for the Pleistocene beds of the sequence using the amino acids D-alloisoleucine/L-isoleucine (A/I) in the molluscan species *T. spissa* and *Austrovenus stutchburyi*. This work demonstrated the utility of the technique in combination with tephrochronology and MIS periodicity, and it showed that the two venerid bivalves racemize at similar rates.

Our four Whanganui samples were collected from three locations along the coast.

1. Coastal bluffs along Castlecliff Beach (site 11 of Bowen et al., 1998) expose gently dipping early to middle Pleistocene marine strata whose ages are well constrained

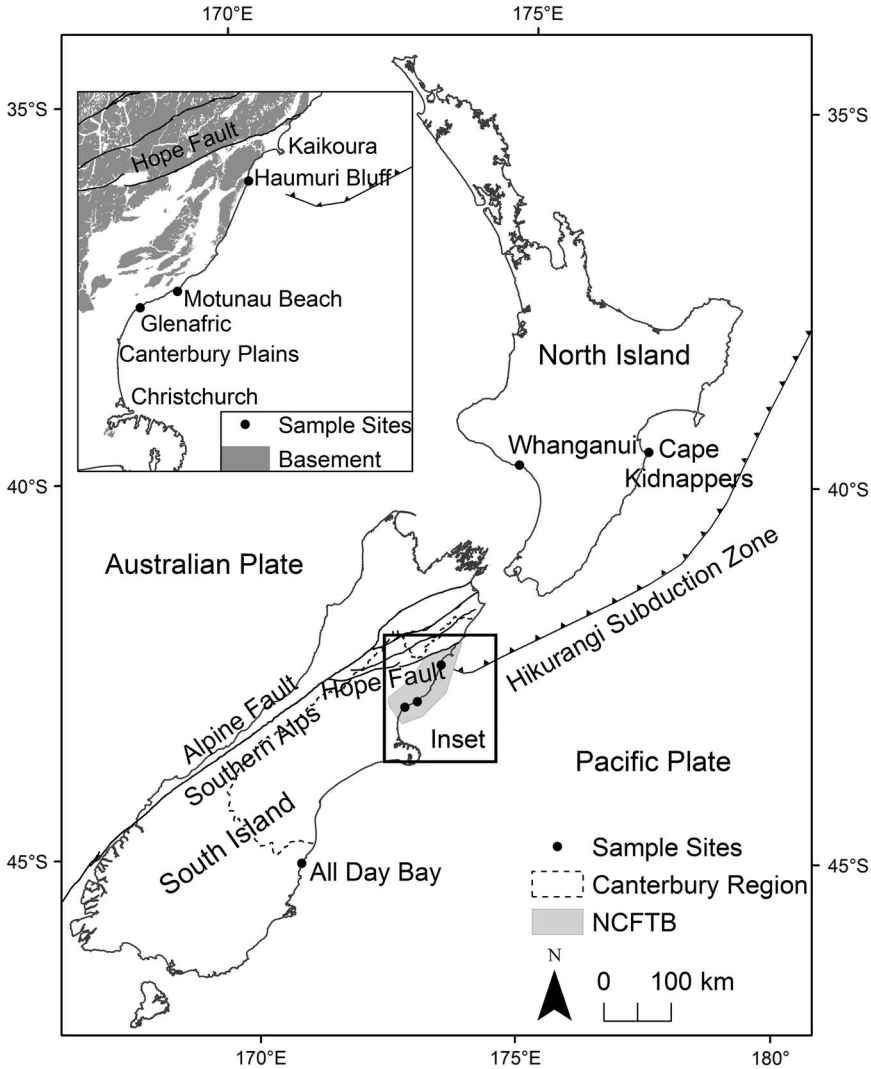

Figure 1. Major features of the New Zealand plate boundary showing sampling sites. Haumuri Bluff, Motunau Beach, and Glenafric are the sites of marine terraces within the North Canterbury fold-and-thrust belt (NCFTB) that were dated in this study. Cape Kidnappers, Whanganui, and All Day Bay were sampled for the amino acid racemization calibration. The extent of basement rocks in the inset is from Rattenbury et al. (2006) and Forsyth et al. (2008).

https://doi.org/10.1017/qua.2016.9 Published online by Cambridge University Press

by multiple lines of evidence including tephrochronology (Kohn et al., 1992; Alloway et al., 1993; Shane et al., 1996; Pillans et al., 2005) and cyclostratigraphy (Beu and Edwards, 1984; Carter and Naish, 1998; Naish et al., 1998). We collected *T. spissa* and other taxa from the Kupe Formation (MIS 17) and the Shakespeare Cliff Sand (MIS 11). Samples from several of the older formations at Castlecliff Beach were also analyzed for AAR (Supplementary Table 2), but no *T. spissa* shells were found and data are not included in the calibration.

2. Road and river cuts near the mouth of Whanganui River at Landguard Bluff expose a complicated stratigraphy of marine and terrestrial sediment (Pillans et al., 1988). We sampled *T. spissa* and other taxa from the Waipuna Delta Conglomerate (site 4 of Bowen et al., 1998), which is correlated with the Ngarino marine terrace (Beu and Edwards, 1984). An MIS 7c age for the conglomerate has been established by Pillans et al. (1988) on the basis of stratigraphy, paleontology, and identification of a tephra of known age.
3. Also in the Whanganui area, sediments underlying the Hauriri marine terrace are exposed at Waverley Beach (site 2 of Bowen et al., 1998) where they have been correlated with MIS 5a (Pillans, 1983) based on their elevation relative to terraces of known age.

Our other samples were collected from two sites not within the Whanganui Basin.

1. Approximately 150 km to the east, an uplifted marine terrace at Cape Kidnappers (site 1 of Bowen et al., 1998) exposes Holocene marine sediment with *T. spissa* shells that were previously radiocarbon dated to around 2.5 ka (Hull, 1987). Although we could not relocate *T. spissa* shells, we collected shells of *Venerupis largillierti* and analyzed them for both AAR and radiocarbon.
2. In the Otago region on the South Island, we collected *T. spissa* shells at about 3 meters above sea level (m asl) exposed in a coastal bluff at All Day Bay underlying a prominent terrace. Given its elevation, the fact that this segment of coast is tectonically stable (Pillans, 1990), and the presence of other MIS 5e terraces in this area (Pillans, 1990), an MIS 5e age is indicated for this sample.

North Canterbury marine terraces—tectonic setting and previous work

The North Canterbury terraces lie within the North Canterbury fold-and-thrust belt, a distinct structural domain within the larger Canterbury region (Pettinga et al., 2001). The fold-and-thrust belt lies on the Pacific plate near the transition between the Hikurangi subduction zone, which forms the plate boundary to the north, and the trans-pressive Alpine Fault, which forms the plate boundary through most of the South Island (Fig. 1). It is bounded to the north by the strike-slip Hope Fault, to the west by the Southern Alps, and to the south by the Canterbury Plains (Pettinga et al., 2001).

Marine terraces (Fig. 2) occur along much of the coastline within the fold-and-thrust belt, most prominently on the limbs of actively growing, basement-cored anticlines. Typically, there is one wide terrace, from several hundred meters to as much as 3.5 km in width (Fig. 2a and b), with two or three smaller, more dissected terrace remnants above it (Carr, 1970; Yousif, 1987; Barrell, 1989). The marine terraces of North Canterbury were first systematically described by Jobberns (1926, 1928) and Jobberns and King (1933). These early works established the marine origin of the terraces. Carr (1970) mapped terraces in the southern part of North Canterbury and proposed correlations with

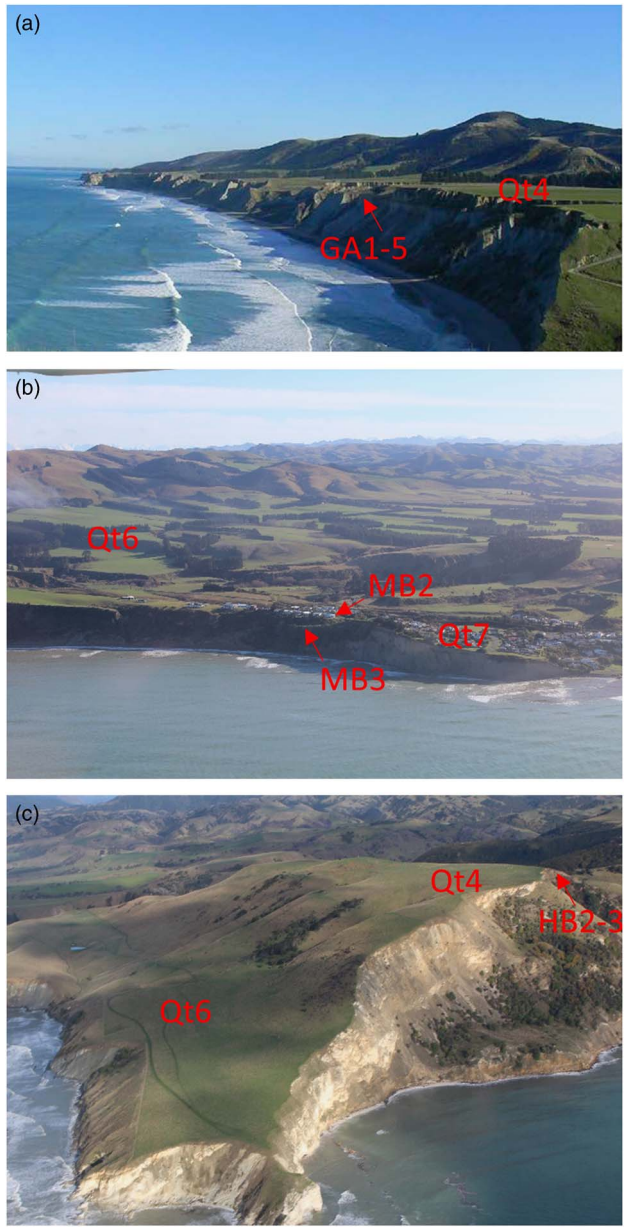

Figure 2. (color online) Aerial views of marine terraces at the following: (a) Glenafric; view is to the south. (b) Motunau Beach; view is to the west. (c) Haumuri Bluff; view is to the south. Sample sites (GA, MB, and HB) and terrace units (Qt) are labeled.

https://doi.org/10.1017/qua.2016.9 Published online by Cambridge University Press

interglacial periods of Suggate (1965). Bull (1984) correlated the terraces at Kaikoura Peninsula with the U-series-dated New Guinea terrace sequence of Bloom et al. (1974) and Chappell (1983), based on the altitudinal spacing of the terraces. Yousif (1987) used remote sensing to map terraces and assigned ages based on correlation to sea-level high stands, using relative elevation, relationships to fluvial aggradation gravels inferred to date from periods of glacial advance, and proposed correlations between knick points and terraces. Barrell (1989) mapped and proposed ages for terraces in the vicinity of Motunau Beach based on elevation and correlation to sea-level high stands. Ota et al. (1984, 1996) were the first to apply numerical geochronological techniques (AAR and ^{14}C) to the North Canterbury terraces, working in the northern part of the area. Most recently, terraces capped by marine deposits were mapped at 1:250,000 scale (Rattenbury et al., 2006; Forsyth et al., 2008) and were assigned to MISs on the basis of elevation and degree of dissection. Table 1 summarizes the ages assigned to the terraces in these previous studies.

The AAR dating by Ota et al. (1996) and ^{14}C dating by Ota et al. (1984) are the only numerical ages for the North Canterbury terraces (Table 1). Previous luminescence dating in the Canterbury region has focused on loess (Berger et al., 2001; Almond et al., 2007) and glacial or glaciofluvial sediments (Rother et al., 2010; Shulmeister et al., 2010; Rowan et al., 2012), although IRSL dating has proved useful in dating marine sediments in North Westland (Rose, 2011). The previous work in Canterbury has shown promise but also difficulties for the technique (Rowan et al., 2012), including some age reversals in loess IRSL ages (Berger et al., 2001; Almond et al., 2007). Feldspar IRSL, which we use in this study, does not suffer from the low signal intensities observed in quartz in this region (Rowan et al., 2012). It can be susceptible to anomalous fading (Huntley and Lamothe, 2001; Huntley and Lian, 2006), but this phenomenon has not been observed in previous South Island studies (Almond et al., 2001; Hormes et al., 2003; Preusser et al., 2005; Rother et al., 2010; Shulmeister et al., 2010; Rose, 2011). Given the scarcity of numerical ages for the North Canterbury marine terraces, we dated samples from three locations along the North Canterbury coast, where marine terraces are prominent: Glenafric, the Motunau Beach area, and Haumuri Bluff (Fig. 3).

Glenafric

At the southern end of the North Canterbury fold-and-thrust belt near Glenafric Beach and the adjacent Glenafric farm, marine terraces are uplifted along the limb of a small anticline (Fig. 3a), named the Kate anticline (Wilson, 1963; Yousif, 1987). The most extensive marine terrace at this site (Qt4 in Fig. 3a) is termed the Tiromoana terrace after Carr's (1970) name for the Quaternary sediments (marine and terrestrial) that overlie the wave-cut platform in this area. It is tilted up to the northeast (Fig. 2a), with the terrace tread rising from about 45 m to about 80 m in elevation over a distance of ~6 km. The bedrock strath is overlain by marine sand and gravel, alluvium, and loess (Fig. 4). Previous age estimates for the terrace have ranged from MIS 3 to 5 (Table 1), although it has not been numerically dated. Remnants of higher terraces form small notches and hilltops and have been grouped into two (Carr, 1970) or three (Yousif, 1987) additional terraces on the basis of elevation.

We collected two IRSL samples from the principal terrace (Qt4), one from the marine sediment and one from the overlying loess (Fig. 4). We collected *T. spissa* shells for AAR analyses from the same site as the marine sediment IRSL sample and from an additional site on the same terrace and same stratigraphic position a few tens of meters away. Sample sites are shown in Figure 3a.

Motunau Beach

An extensive marine terrace occupies the coast from south of Motunau Beach north to Stonyhurst Creek (Figs. 2b and 3b, terrace Qt6), along one limb of the Montserrat anticline. At up to 3.5 km wide, this terrace is the widest in North Canterbury. The marine and terrestrial sediments overlying the wave-cut bench were termed the Motunau Formation by Carr (1970), and the terrace has been termed the Motunau Coastal Plain or Motunau Terrace (Jobberns and King, 1933; Carr, 1970; Barrell, 1989). Previous age estimates have varied, with most work assigning its formation to sometime in MIS 5 (Table 1), but again there has been no numerical dating. As at Glenafric, higher terraces are preserved as notches in the hillside, which were grouped into two levels by Yousif (1987) and three by Barrell (1989), but suitable materials were not found for dating.

We collected two IRSL samples from marine sand of the main terrace where the overlying sediments (Fig. 4) are exposed in road cuts. One sample (MB2) was taken near Motunau Beach village and the other (MB1) at Boundary Creek (Fig. 3b). *T. spissa* shells for AAR analyses were collected from four sites near the southwest end of the terrace (Fig. 3b), from between 0.3 and 2.8 km from the former sea cliff.

Haumuri Bluff

Haumuri Bluff is the northernmost of our three North Canterbury study sites. Two prominent marine terraces (Qt4 and Qt6 in Fig. 3c), capped by marine sediments and loess, are found at this location, and their correlatives have been mapped along the coast to the south (Ota et al., 1984) on the flanks of the Hawkswood anticline. Ota et al. (1996) dated the upper terrace (Tarapuhi terrace/Qt4) to MIS 5c on the basis of an AAR age of 135 ± 35 ka and the presence of a cold-water molluscan fauna considered to be incompatible with MIS 5e. Correlating to the sea-level curve of Chappell and Shackleton (1986), they gave this terrace an age of 100 ± 3 ka and assigned the lower of the two prominent terraces (Amuri

https://doi.org/10.1017/qua.2016.9 Published online by Cambridge University Press

Table 1. Names and ages of marine terraces based on previous work and this study.

Glenafric						Motunau Beach								Haumuri Bluff								This study	
Carr (1970)		Yousif (1987)		QMAP[b]		Carr (1970)		Yousif (1987)		Barrell (1989)		QMAP		Ota et al. (1984, 1996)			Warren (1995)	QMAP					
Name	Age[a]	Name	Age (ka)	Name	Age (MIS)	Name	Age[a]	Name	Age (ka)	Name	Age (ka)	Name	Age (MIS)	Name	1984 Age[a]	1996 Age (ka)	Name	Name	Age (MIS)			Name	Age (MIS)
Leonard Formation	Waiwheran	M4	125	mQb	6–13					Vulcan Terrace 3	210	mQb	6–13									Qt1	7c
Leonard Formation	Waiwheran	M3	105	mQb	6–13	Stonyhurst Formation	Waiwheran	M4	125	Vulcan Terrace 2	118–124	mQb	6–13									Qt2	7a
Bob's Flat Formation	Terangian	M2	80	mQb	6–13	Stonyhurst Formation	Waiwheran	M3	105	Vulcan Terrace 1	106	Q7b mQb	7 6–13									Qt3	5e
Tiromoana Formation	Oturian	M1	60	Q5b	5									Tarapuhi Terrace	Waiwheran	100 ± 3	TrigT Formation	Q9b	9			Qt4	5c
														Kemps Hill Terrace	Terangian	81 ± 3 (upper) 72 ± 3 (lower)	Kemps Hill Formation	Q7b	7			Qt5	5a-c
						Motunau Formation	Terangian-Waimean	M2	80	Motunau Terrace	83	Q5b	5	Amuri Bluff Terrace	Oturian	59 ± 3	Wenlock Formation	Q5b	5			Qt6	5a
						Estuarine Beds	Oturian-Otiran															Qt7	3
Amberley Formation	Aranuian	M0	Holocene	Q1b	1									Conway Flat Terrace	Holocene (ca. 8 ka)		Rafa Formation	Q1b	1			Qt8	1

Notes: Gray boxes indicate that a terrace is not present in a given area or was not described by a given study. MIS, marine isotope stage.
[a]Terrace ages from Carr (1970) and Ota et al. (1984) use the glacial-interglacial stage names of Suggate (1965). From youngest to oldest, the interglacials are Aranuian (present), Oturian, Terangian, and Waiwheran.
[b]QMAP (quarter million mapping program) geologic maps covering this area are Rattenbury et al. (2006) and Forsyth et al. (2008).

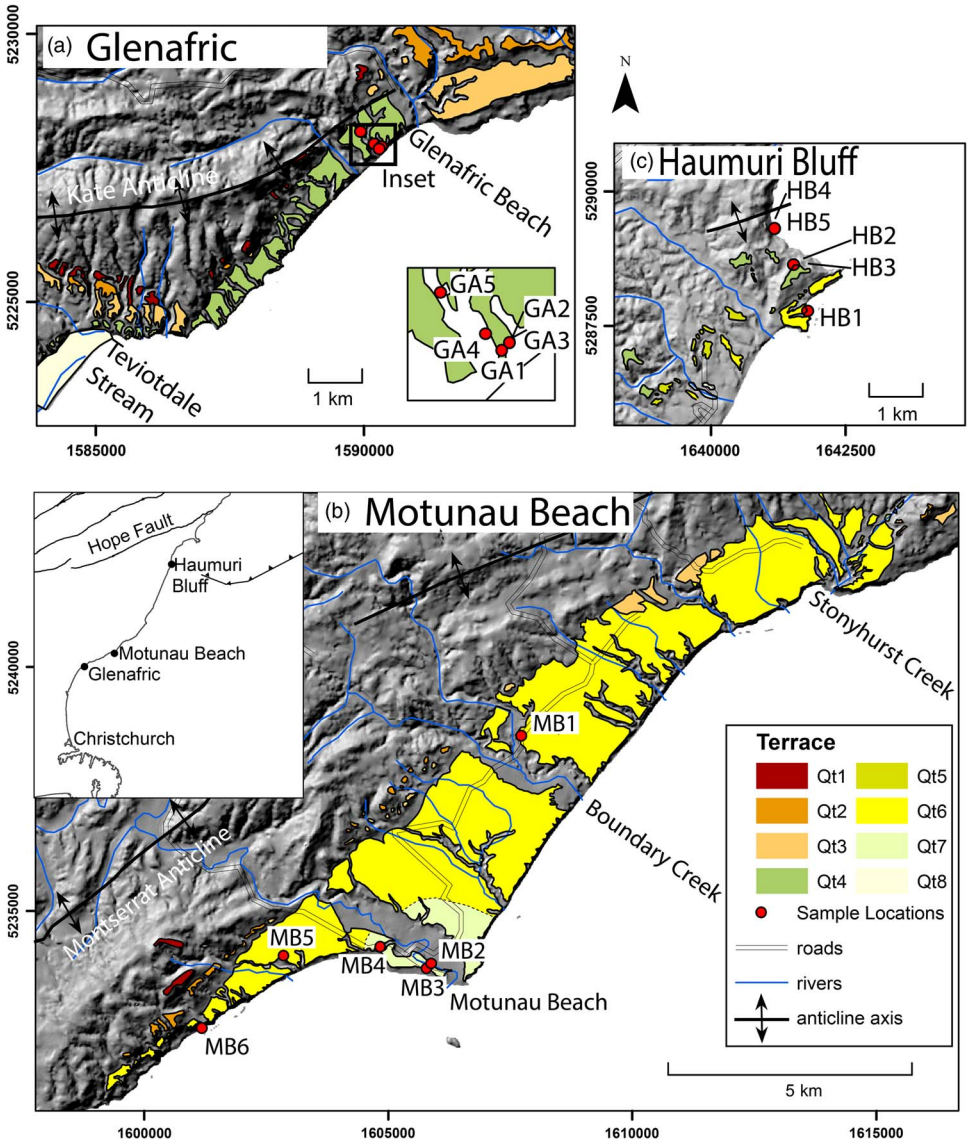

Figure 3. (color online) Three North Canterbury field sites: Glenafric (a), Motunau Beach area (b), and Haumuri Bluff (c). Mapping of terraces is based on previous maps by Yousif (1987), Barrell (1989), Warren (1995), Pettinga and Campbell (2003), Rattenbury et al. (2006), and Forsyth et al. (2008); unpublished QMAP (quarter million mapping program) record sheets provided by GNS Science (http://data.gns.cri.nz/metadata/srv/eng/search); and interpretation of aerial photographs from Land Information New Zealand. The background is a hill shade of the 10 m DEMs (digital elevation models) from Rattenbury et al. (2006) and Forsyth et al. (2008).

Bluff terrace/Qt6) to 59 ± 3 ka, based on the same sea-level curve, given the presence of another terrace (Kemps Hill terrace) immediately to the southwest (Table 1 and Fig. 3c), which is between the Tarapuhi and Amuri Bluff terraces in elevation.

We collected samples for IRSL dating from the marine sediments on both Tarapuhi (Qt4) and Amuri Bluff (Qt6) terraces, and we collected shells for AAR analyses from the Tarapuhi terrace at the location sampled by Ota et al. (1996) (Figs. 3c and 4). In addition, we found a small terrace at about 4.2 m elevation cut into the Torlesse basement rock northwest of Haumuri Bluff (Fig. 3c), which we call the Torlesse terrace. *Leukoma crassicosta* shells from this terrace were sampled for ^{14}C and AAR analyses.

METHODS

IRSL

IRSL samples were collected from sand and silt lenses or layers within the marine sand and gravel units of the terraces, or in the case of sample GA1, from loess. A metal tube was inserted into the sediment to collect each sample. The ends of the tube were then covered with aluminum foil, and the tube was wrapped in black plastic and taped shut to ensure darkness and moisture retention. For coastal and eolian sediments, the luminescence signal is generally reset by exposure to sunlight during deposition (Kaufman et al., 1996; Singarayer et al., 2005), although incomplete resetting or

https://doi.org/10.1017/qua.2016.9 Published online by Cambridge University Press

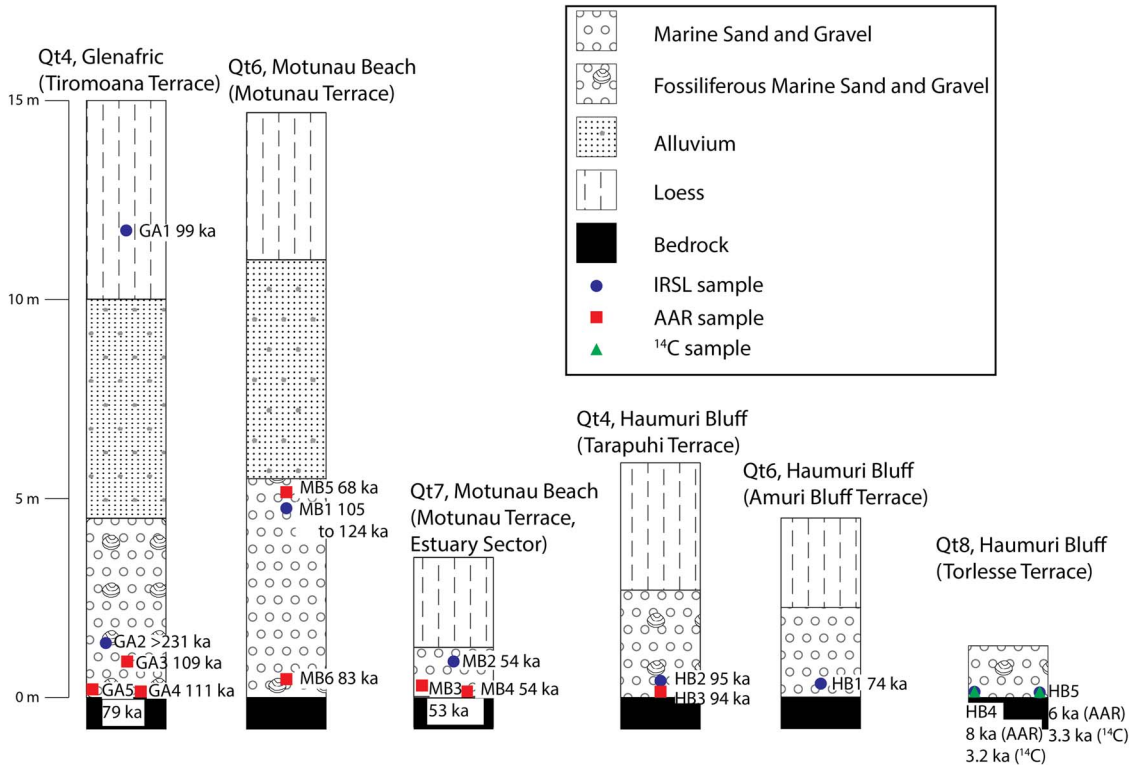

Figure 4. (color online) Representative stratigraphy for the marine terraces dated in this study, showing the locations of samples relative to the bedrock surface. The thickness of stratigraphic units varies laterally on each terrace, including between sample sites. Stratigraphic columns are based on Carr (1970), Ota et al. (1996), and this study. For uncertainties in ages, see Tables 2, 3, and 5.

nonresetting was considered for samples that produced anomalously old ages.

IRSL dating of feldspar grains was conducted by the Luminescence Dating Laboratory at Victoria University, Wellington, using the single aliquot regenerative method, as described by Murray and Wintle (2000). The blue luminescence of fine-grained (4–11 µm) feldspar was measured during infrared stimulation. Preheating was done at 270°C for 30 s. Blue luminescence centered at about 410 nm was detected using an EMI 9235QA photomultiplier with Schott BG39 and Kopp5-58 filters. Preheating and the use of 410 nm blue luminescence overcomes the potential age underestimation caused by the thermally unstable 290 nm emissions peak (Krbetschek et al., 1996; Clarke and Rendell, 1997), which has been an issue for some samples from Westland, New Zealand (Rose, 2011), for which UV luminescence was measured instead. Fading tests were performed using the method of Huntley and Lamothe (2001), but no anomalous fading was detected. Equivalent dose (D_e) values were determined for 8 or 12 aliquots, and the arithmetic mean of these was used for the age calculation.

Dose rates were determined from radionuclide content, water content, and *a*-value and from the expected dose rate from cosmic rays. Radionuclide contents were measured in the laboratory using gamma spectrometry. Gamma rays were counted for a minimum of 24 h, using a high-resolution, broad-energy gamma spectrometer. Spectra were analyzed with GENIE2000 software. U, Th, and K concentrations were determined by comparison to standard samples. The dose rate from radionuclides was calculated from the activity concentrations of ^{40}K, ^{208}Tl, ^{212}Pb, ^{228}Ac, ^{214}Bi, ^{214}Pb, and ^{226}Ra, using the conversion factors of Guérin et al. (2011). Water content for each sample was calculated as the weight of water divided by dry weight of the sample, with an assumed 25% uncertainty. The *a*-value, a measure of the contribution of alpha radiation to the luminescence signal (Aitken and Bowman, 1975), was estimated at 0.05 ± 0.01 for all samples. The dose rate from cosmic rays was calculated from burial depth, geomagnetic latitude, and altitude, using the formulas and correction factors of Prescott and Hutton (1994).

AAR

Shells of marine bivalve mollusks of the family Veneridae were chosen for the analysis, with the species *T. spissa* used wherever possible. This species is common in New Zealand (Powell, 1979) and has proved suitable for use in previous AAR studies (Ota et al., 1996; Bowen et al., 1998). Additional analyses were conducted on some other marine mollusk species, which provide a supporting data set for both the calibration and the previously undated samples (Supplementary Table 2). AAR analyses were conducted at the Northern Arizona University Amino Acid Geochronology Laboratory using reverse-phase high-performance liquid chromatography (HPLC) (Kaufman and Manley, 1998). Ratios of right- (D) and left-handed (L) isomers were measured for eight amino

https://doi.org/10.1017/qua.2016.9 Published online by Cambridge University Press

acids: aspartic acid (Asp), glutamic acid, serine (Ser), alanine (Ala), valine, phenylalanine, isoleucine, and leucine (Leu). In contrast, Ota et al. (1996) and Bowen et al. (1998) used ion-exchange HPLC, which focuses entirely on A/I. Our results are not quantitatively comparable to the previously published results for this reason and because we pretreated the shells to isolate the intracrystalline fraction of amino acids, following the techniques of Penkman et al. (2008).

AAR calibration curves were calculated using the Bayesian fitting method and R scripts of Allen et al. (2013). We tested four different functions for relating sample age to D/L ratio: apparent parabolic kinetics (APK) (Mitterer and Kriausakul, 1989), simple power-law kinetics (SPK) (Goodfriend et al., 1995), constrained power-law kinetics (CPK) (Manley et al., 2000), and time-dependent reaction kinetics (TDK) (Allen et al., 2013). For each function, we tested two possibilities for the D/L value at time 0 (R_0): that it is fixed at 0 and that it is allowed to vary as a fitted parameter (denoted by 0 or 1, respectively, after the function name). For the uncertainty in the age predicted from the D/L ratio, we tested both lognormal and gamma distributions, as suggested by Allen et al. (2013). Of the eight amino acids measured, Ser was not used because its D/L ratio did not increase monotonically with age, and the TDK and CPK models were not tested for Ala and Leu because we measured D/L values greater than 1 for these amino acids. In total, 96 combinations of amino acid, age-D/L function, and probability distribution were tested. Following the methods described in Allen et al. (2013), we used the Bayesian information criterion (BIC) (Schwarz, 1978) to identify a best-fit model and for Bayesian model averaging (Hoeting et al., 1999), which included all models within 6 BIC units of the best-fit model (Allen et al., 2013).

Radiocarbon

Holocene shells from two locations were analyzed for ^{14}C in order to date the young terraces and to help calibrate the rate of AAR. These included analyses using gas proportional counting by Beta Analytic, and accelerator mass spectrometry (AMS) using both graphite targets for full-precision ages and carbonate targets for lower-precision ages (Bush et al., 2013) at the University of California, Irvine, Keck Carbon Cycle AMS facility. Radiocarbon ages were calibrated using Calib 7.0.4 and the Marine13 (Reimer et al., 2013) database. We used a ΔR value of 25 ± 35 ^{14}C yr (http://calib.qub.ac.uk/marine/; Higham and Hogg, 1995) for the North Canterbury samples and -25.8 ± 15 ^{14}C yr (Higham and Hogg, 1995) for the Cape Kidnappers samples.

RESULTS

IRSL

The IRSL ages (Table 2) indicate the marine terraces formed during various stages of the last interglacial cycle, with most corresponding to substages of MIS 5 (Fig. 5) We use 2 standard error uncertainties in order to compare these results to the 95% confidence intervals for the AAR ages. For sample GA2, from the beach facies at Glenafric, the luminescence growth curve approached saturation, resulting in a minimum age estimate far older than any of the other samples. This indicates that the luminescence signal of the sediment had not been zeroed during transport and is unlikely to reflect the true age of the terrace. Sample MB1 showed disequilibrium in the uranium decay chain, which affects the estimated dose rate and thus the age of the sample. Three different ages (Table 2) have been calculated for this sample using three different estimates of uranium content, based on (1) ^{234}Th; (2) ^{226}Ra, ^{214}Pb, and ^{214}Bi; and (3) ^{210}Pb.

Radiocarbon

The ^{14}C results (Table 3) support late Holocene ages for samples from the low-elevation terraces at Cape Kidnappers and Haumuri Bluff. At Cape Kidnappers, one shell from sample CK4 was dated at 529–455 and 515–325 cal yr BP and is significantly younger than the previously determined age of 2300 cal yr BP for the terrace (Hull, 1987). We assume that the shells in our collection were deposited on top of the terrace following its abandonment, perhaps by storm waves. These shells were

Table 2. Analytical data used to calulate luminesence ages.

Sample number	Laboratory code (WLL-)	Depth below surface (m)	Water content (%)	U[a] (ppm)	Th (ppm)	K (ppm)	Cosmic ray dose rate (Gy/ka)	Total dose rate (Gy/ka)	D_e (Gy)	Luminescence age (ka) (2 SE)[b]
GA1	1113	3.5	12.5	2.55 ± 0.15	8.01 ± 0.11	1.63 ± 0.04	0.1310 ± 0.0066	3.19 ± 0.15	314.86 ± 4.60	99 ± 9
GA2	1083	6	0.202	2.09 ± 0.17	8.71 ± 0.14	1.99 ± 0.05	0.0970 ± 0.0048	3.15 ± 0.18	>728.85 ± 15.53	>231 ± 28[c]
MB1[d]	1112	4	15.6	1.40 ± 0.14	4.27 ± 0.06	1.39 ± 0.03	0.1230 ± 0.0062	2.18 ± 0.11	270.90 ± 3.94	124 ± 13
				2.01 ± 0.10				2.37 ± 0.12	270.90 ± 3.94	114 ± 12
				2.68 ± 0.15				2.57 ± 0.13	270.90 ± 3.94	105 ± 12
MB2	1082	2.5	0.136	1.40 ± 0.17	4.55 ± 0.07	1.55 ± 0.03	0.1490 ± 0.0075	2.40 ± 0.10	130.0 ± 4.4	54 ± 6
HB1	1114	4.4	22.5	2.21 ± 0.15	9.44 ± 0.13	2.39 ± 0.05	0.1171 ± 0.0059	3.53 ± 0.21	260.82 ± 3.04	74 ± 9
HB2	1109	5.3	15.2	1.98 ± 0.15	8.09 ± 0.09	2.09 ± 0.04	0.1051 ± 0.0053	3.33 ± 0.16	316.50 ± 6.12	95 ± 10

[a]U content was calculated in three ways: from ^{234}Th; from ^{226}Ra, ^{214}Pb, and ^{214}Bi; and from ^{210}Pb. For samples for which the three values are within error of each other, only the median value is given here. For MB1, all three are given (in the order listed here).
[b]Uncertainties of 1 standard error (SE) were reported by the luminescence laboratory. However, we use 2 SE uncertainties in the text for comparison with the 95% confidence intervals on the AAR ages.
[c]This is a minimum age. The growth curve for sample GA2 trends toward saturation.
[d]Uranium decay chains were in disequilibrium for sample MB1. Three different ages are calculated based on three different uranium concentrations.

https://doi.org/10.1017/qua.2016.9 Published online by Cambridge University Press

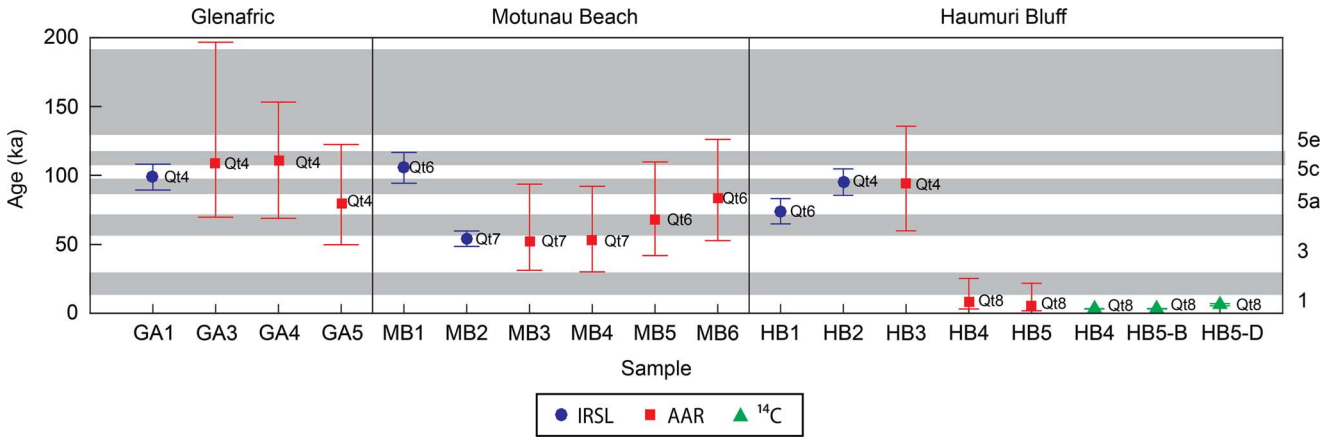

Figure 5. (color online) Sample age estimates for the three study areas in relation to marine isotope stages. Interstadials are white; stadials are shaded. Stage boundaries are from Lisiecki and Raymo (2005), and substage boundaries are from Williams et al. (2015). Error bars represent 95% confidence intervals for amino acid racemization (AAR) calibration curves, 2 standard errors for infrared-stimulated luminesce (IRSL), and 2-sigma range of calendar-year calibrations for radiocarbon ages (^{14}C). Labels next to points indicate the terrace designation in Table 1 for this study. Data are listed in Tables 2, 3, and 5.

collected from sand about 1–2 m above the bedrock contact, so they may not be comparable to Hull's (1987) samples, which were collected from within or immediately above the basal gravel. At Haumuri Bluff, we rejected the ^{14}C age for sample HB5-D as it is inconsistent with samples HB5-B and HB4, which were collected from the same site and the same marine gravel unit, and it consisted of a small shell fragment, which was noted by the laboratory as being very small or nonhomogeneous.

AAR calibration and ages

Six collections of shells were used for the AAR calibration data set (Table 4). The age for the Cape Kidnappers sample is based on our ^{14}C results (Table 3, sample CK4). Although younger than Hull's (1987) age for the terrace, this age is paired with our AAR analyses. The ages for the other five samples are based on their independently determined MIS or substage as described previously, using the midpoint of the age range (Lisiecki and Raymo, 2005; Williams et al., 2015) as the best age and half the age range as the uncertainty, with assumed Gaussian distribution.

Table 3. Results of radiocarbon analyses.

Laboratory code[a]	Laboratory code (UAL)[d]	Sample number	Radiocarbon age (yr BP[e])	Calendar age[g] (yr BP[e])
350130[b]	10174	HB4	3410 ± 30	3371–3121
$CaCO_3$ target	10936-B	HB5-B	3450 ± 35	3420–3162
$CaCO_3$ target	10936-D	HB5-D	5790 ± 350[f]	6993–5409
$CaCO_3$ target	13468-A	CK4-A	785 ± 45	515–325
163843[c]	13468-A	CK4-A	845 ± 15	529–455

[a]$CaCO_3$ targets analyzed at University of California, Irvine (UCI) using the procedure of Bush et al. (2013) are considered range-finder ages and are not assigned a laboratory code.
[b]Beta Analytic code. Analyzed by beta counting. All other samples analyzed by accelerator mass spectrometry (AMS).
[c]UCI AMS code.
[d]Northern Arizona University Amino Acid Geochronology Laboratory identifier.
[e]Years before present, using AD 1950 as the present datum.
[f]This sample was very small and/or inhomogeneous.
[g]Two-sigma age ranges determined using Calib 7.0.4 and the Marine13 database.

The AAR calibration focuses on Asp D/L (Table 4) because the best-fitting models rely on this amino acid, which is among the most abundant in the shells and analytically the most reproducible. The best-fitting model (lowest BIC) is SPK1 with $R_0 = 0.190$ for Asp, with a lognormal distribution, and with coefficient $a = 1.53 \times 10^6$ yr and exponent $b = 4.83$ (Supplementary Table 3). The range of possible SPK models can be used to assign confidence intervals to the predicted ages (Fig. 6). Seven other models are within 6 BIC units from the best-fit model, the cutoff used for Bayesian averaging (Supplementary Table 3). Six of these models also use Asp, and one uses Leu. Four use SPK; two, TDK; and one, CPK. Four use lognormal distributions, and three use gamma distributions.

None of the models within 6 BIC units of the best fit is an APK model. This is in agreement with the results of Allen et al. (2013), who generally found APK to provide a poor fit when using the Bayesian fitting procedure. It should be noted, however, that APK can provide a good fit to the three samples of MIS 5e age or younger. We prefer not to use a model that is such a poor fit to our complete data set, however, when the model that best fits the entire data set is still a good fit to the three youngest data points (Fig. 6). Moreover, we aim to generate an AAR age model that can be applied over as wide a range of ages as possible, and SPK provides this, whereas APK does not.

Differences in temperature history among the samples could account for some of the unexplained variance in the AAR calibration. Specifically, the sample from All Day Bay is from

https://doi.org/10.1017/qua.2016.9 Published online by Cambridge University Press

Table 4. Data set used for amino acid racemization calibration.

Laboratory code (UAL)	Location	Latitude (°)	Longitude (°)	MAT[a] (°C)	n[b]	Asp D/L Mean	Asp D/L Standard deviation	MIS[c]	Median age (ka)	Uncertainty[d] (ka)
13468	Cape Kidnappers	–39.6	177.1	14.6	6	0.220	0.016	1	0.56	0.04
10933	Waverley	–39.8	174.6	14.0	5	0.538	0.014	5a	79	8
9448	All Day Bay	–45.2	170.9	11.1	5	0.606	0.015	5e	123.5	6.5
9433	Landguard	–40.0	175.0	14.0	5	0.644	0.041	7	217	26
9417	Shakespeare Cliff	–39.9	174.8	14.0	5	0.767	0.016	11	399	25
9414	Kupe Formation	–39.9	174.8	14.0	5	0.848	0.007	17	694	18

Note: All analyses on *Tawera spissa* except mollusks from Cape Kidnappers, which are *Venerupis largillierti*, which is in the same family as *T. spissa*. See Supplementary Table 2 for details of individual shells and all amino acids measured.
[a]Mean annual temperature. Data are from NIWA (the National Institute of Water and Atmospheric Research) for the period 1981–2010 from stations closest to the sample site, including Napier for Cape Kidnappers, Whanganui for Landguard, Shakespeare Cliff and Kupe Formation, and Dunedin for All Day Bay. For comparison, the MAT at Christchurch is 12.2°C (http://www.niwa.co.nz/sites/www.dev2.niwa.co.nz/files/sites/default/files/mean_monthly_air_temperature.xlsx).
[b]Number of individual shells analyzed and used to calculate sample mean.
[c]Marine oxygen isotope stages (MISs) based on ages assigned by previous workers, as described in the text.
[d]The 95% confidence, based on ^{14}C results for Cape Kidnappers and MIS for the rest. See text for details.

significantly farther south than the other samples and thus presumably experienced lower postdepositional temperatures, as indicated by the modern temperature (Table 4). Lower temperatures reduce racemization rates, and thus we would expect the D/L value for this sample to be lower than the trend that is largely determined by results from farther north. The best-fit model, in fact, essentially intersects the D/L value for the MIS 5e sample within errors (Fig. 6), so we conclude that the effect of the temperature difference is not significant, and that the calibration model applies to both islands of New Zealand. The sample from Cape Kidnappers likely experienced similar temperatures to Whanganui (Bowen et al., 1998; Table 4), but the shells are of the species *V. largillierti*, which

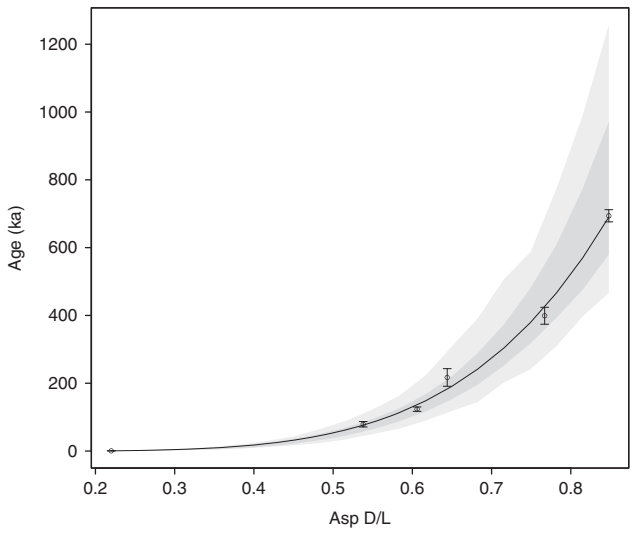

Figure 6. Amino acid calibration curve for racemization of aspartic acid (Asp) based on the best-fitting simple power-law kinetics 1 model and lognormal distribution (Supplementary Table 3). Dark shading represents 95% confidence intervals for mean age, and light shading represents 95% prediction intervals. Data are listed in Table 4.

along with *T. spissa* is in the family Veneridae. Differences in racemization rates among venerid bivalves are estimated at approximately ±10% (Lajoie et al., 1980). To test the sensitivity of the calibration model to possible taxonomic effects, we tried adjusting the D/L value of this sample by ±10%. The differences in predicted ages from these adjusted D/L values are minor compared with the uncertainties in the age prediction.

To calculate the age of each of the 10 previously undated samples, we used the average D/L measurements for that sample (n = 5) and the Bayesian model averaging of age predictions from all models within 6 BIC units of the best-fit model. For each sample, a weighted mean age was calculated, along with a 95% confidence interval (Table 5). These uncertainties, which take into account the eight models with BIC values below the cutoff, are larger than the confidence intervals for SPK1 alone (Fig. 6).

DISCUSSION

Glenafric

The 99 ± 9 ka IRSL age of sample GA1 for the loess on the Qt4 terrace suggests an MIS 5c age for the terrace (Fig. 5). Because the sample was collected from loess, at about 7 m above the top of the marine sediments, its age is a minimum for the terrace. About 5 m of alluvium separates the two layers. Although its rate of deposition is unknown, it was likely deposited rapidly following sea-level retreat, as the low slope of the abandoned terrace would likely have caused aggradation of streams flowing from the adjacent steep hills. Loess accumulation rates are also uncertain, but rates of up to 1 mm/yr have been reported elsewhere in Canterbury (Almond et al., 2007). Given such rates of deposition and the uncertainties in the IRSL age and in the timing of sea-level high stands, this result is consistent with an MIS 5c age for the terrace. An MIS 5e age cannot be entirely ruled out, but there are no obvious stratigraphic unconformities within the cover sediments

https://doi.org/10.1017/qua.2016.9 Published online by Cambridge University Press

Table 5. Amino acid racemization ages.

			Asp D/L				
Laboratory code (UAL)	Sample	n[a]	Mean	Standard deviation	2.5th Percentile (ka)	Estimated age (ka)	97.5th Percentile (ka)
9455	GA3	5	0.576	0.016	70	109	197
10938	GA4	5	0.585	0.015	69	111	153
10937	GA5	5	0.542	0.043	50	79	122
10929	MB3	5	0.495	0.019	32	53	94
10928	MB4	5	0.500	0.012	30	54	92
10930, 10932	MB5	5	0.524	0.027	42	68	109
10931	MB6	5	0.548	0.017	53	83	126
10175, 10178	HB3	5	0.564	0.025	60	94	136
10174	HB4	5	0.319	0.024	3	8	25
10936	HB5	5	0.289	0.018	2	6	22

[a]Number of individual shells analyzed and used to calculate sample mean.

(Fig. 4), suggesting continuous deposition. The three AAR samples from the marine sand and gravel overlying the bedrock strath produce age estimates ranging from 111^{+42}_{-42} to 79^{+43}_{-29} ka (95% confidence intervals) (Table 5). The youngest (GA5) is most consistent with an MIS 5a age, although the uncertainty overlaps with MIS 5c or 5e as well. This sample exhibits unusually high intershell variability (Table 5), and moreover, MIS 5a is younger than the IRSL age of overlying loess. The other two age estimates lie between MIS 5c and 5e, with uncertainties large enough to encompass both substages. One possibility is that the samples date to MIS 5c but could include shells reworked from substage 5e. The Asp D/L values for this terrace (average of 0.568 for the three samples) are very close to those of the Tarapuhi terrace at Haumuri Bluff (average of 0.564), suggesting that they are the same age, and the age of the latter terrace is more confidently established at MIS 5c (see "Haumuri Bluff" section).

Given the evidence from both IRSL and AAR data, an MIS 5c age is most likely for the main terrace (Tiromoana terrace) at Glenafric. The 60 ka (MIS 3) age estimate of Yousif (1987), which was based on elevation relative to other terraces, is therefore likely too young, and no MIS 3 terrace appears to be preserved at this location. If the youngest terrace was formed during MIS 5c, then higher terrace remnants identified by Carr (1970) and Yousif (1987) may represent MIS 5e and MIS 7 (Table 1).

Motunau Beach

Both the IRSL data (Table 2) and AAR data (Table 5) suggest that at least two different ages of marine sediment are represented by the Motunau Beach samples (Fig. 5), despite the fact that they were all collected from the Motunau coastal plain, which appears nearly continuous on its surface. The 54 ± 6 ka IRSL age for sample MB2 suggests an MIS 3 age for this marine unit (Qt7). AAR samples MB3 and MB4, which were collected near MB2, support this interpretation, with estimated ages of 53^{+41}_{-21} and 54^{+38}_{-24} ka. AAR samples MB5 and MB6, on the other hand, have estimated ages of 68^{+42}_{-26} and 83^{+43}_{-30} ka, which suggest MIS 5a, although MIS 3 or 5c cannot be ruled out given the range of error for those samples. IRSL sample MB1 gives a range of possible ages because of disequilibrium in the uranium decay chain (Table 2). Such disequilibrium can occur as a result of addition or removal of a mobile daughter product within the decay chain and can lead to overestimation of the sample age (Olley et al., 1996). This age range is consistent with an MIS 5e or 5c age for the sample. It is inconsistent with IRSL sample MB2 and AAR samples MB3 and MB4 (Fig. 5). The age for MB1 lies within the 95% confidence intervals of MB6 and MB5, but a younger age for the AAR samples is more likely. Given the AAR data for the other Motunau Beach samples, the youngest of the three possible ages calculated for MB1 (105 ± 12 ka) is the most likely, but the discrepancy between the two dating methods is larger here than at our other sites.

The contrast in ages between the older samples (MB1, MB5, and MB6) and the younger samples (MB2, MB3, and MB4) suggests partial reoccupation of the seaward edge of an older (MIS 5) terrace during the MIS 3 high stand. In this scenario, the lowest, seawardmost part of the older terrace was transgressed during the MIS 3 high stand, but this transgression did not reach the previous sea cliff. Such partial reoccupation can occur when a sea-level high stand reaches the level of the lower part of a previously formed terrace but does not reach all the way to the previous inner edge (Kelsey and Bockheim, 1994). At Motunau Beach, reoccupation occurs only near the seaward edge of the widest terrace within North Canterbury. Alternately, a terrace may have been incised into the lower part of the MIS 5 terrace during MIS 3, but close enough in elevation to the older terrace tread that if any sea cliff formed, it was buried by subsequent colluvial processes and no riser was preserved. These interpretations are in agreement with Carr (1970), who first suggested that the Motunau coastal plain may preserve the record of two marine transgressions.

https://doi.org/10.1017/qua.2016.9 Published online by Cambridge University Press

The older part of the terrace, before reoccupation or incision, would have formed during either MIS 5a (preferred age from AAR samples MB5 and MB6) or MIS 5c-e (IRSL age MB1). The IRSL age is suspect because of the disequilibrium of the U-decay chain, and even the youngest of our three age estimates for this sample might be too old. Further, given the reoccupation or incision of the terrace during MIS 3, an MIS 5c or MIS 5e age for the main terrace would be improbable, and MIS 5a would be more likely. Based on this consideration, the AAR results, and the problematic IRSL results from MB1, we prefer an MIS 5a age for the terrace.

Partial reoccupation of the seaward edge of an MIS 5a terrace during the MIS 3 sea-level high stand is surprising in an uplifting tectonic setting. In this case, however, it is possible given the slope of the MIS 5a terrace and the sea level at this time. The farthest inland MIS 3 sample, MB4, was collected at an elevation of 40 m, immediately on top of the wave-cut platform. Sample MB5, from the MIS 5a terrace, was at 70 m elevation, above a wave-cut platform at 67 m. (MB2 and 3 are offset by a small fault, and MB6 is slumped, so those samples are not useful for this analysis.) The two samples are 1.2 km apart as measured perpendicular to the terrace tread, for a slope of 1.3°, which is low enough to be the original slope of a marine terrace (Trenhaile, 2002), although some tectonic tilting cannot be ruled out. Extrapolating this slope inland to the terrace riser (600 m from MB5) would put the buried shoreline angle of the terrace at about 80 m. The actual elevation may be as high as 100 m because of a steeper slope near the inner edge (Carr, 1970), but this has been attributed to tectonic warping (Carr, 1970; Barrell, 1989), although control on the bedrock elevation near the inner edge is poor away from the Motunau River. Thus, the MB4 sample site was likely at ~40 m below the sea level at the peak of MIS 5a or about −60 m relative to modern sea level, possibly more if the steep slope near the inner edge is not tectonic in nature. Taking a typical age of about 80 ka for MIS 5a and assuming a constant rate of uplift, the sample site would then have been at about −35 m at 60 ka and −23 m at 50 ka. Estimates of MIS 3 sea levels vary widely, with extremes ranging from at or above present-day levels to −85 m (Rodriguez et al., 2000). Our results are consistent with other evidence for relatively high sea levels of −20 to −35 m in New Zealand (Pillans, 1983; Berryman, 1993; Rose, 2011) and southern Australia (Cann et al., 1993; Murray-Wallace et al., 1993) and for similar sea levels in a number of locations worldwide (e.g., Cabioch and Ayliffe, 2001; Mallinson et al., 2008; Wright et al., 2009; Doğan et al., 2012; Wang et al., 2013). They are, however, higher than MIS 3 sea levels inferred from the Huon Peninsula terrace record (Chappell et al., 1996; Yokoyama et al., 2001; Chappell, 2002), for which the highest MIS 3 sea level is −46 to −35 m at 51.8 ± 0.8 ka (Chappell, 2002), as well as most oxygen isotope records (Siddall et al., 2008). If MIS 3 sea level at Motunau Beach did not exceed these lower levels, then the simplest explanation for our results would be that uplift rates have been higher since MIS 3 than between MIS 5a and MIS 3.

The location of the inner edge of the Motunau Beach terrace appears to be lithologically controlled (Jobberns, 1928), coinciding with the more resistant lower part of the Mt. Brown Formation and the Waikari Formation. As such, multiple sea-level high stands likely reached a similar extent inland, each eroding away previously formed terraces. The MIS 5a terrace may have overprinted the 5c terrace in this manner, whereas the lower sea level of MIS 3 was not able to reach as far inland. Above the main terrace, aligned notches and hilltops suggest older terrace remnants (Carr, 1970; Yousif, 1987; Barrell, 1989). We tentatively correlate these with similar remnants at Glenafric (Table 1), which we have assigned to MIS 5e and 7.

Haumuri Bluff

Both IRSL and AAR data support an MIS 5c age for the Tarapuhi terrace (Qt4, Fig. 5), which is in agreement with Ota et al. (1996). The difference between the two ages is only 1 ka, well within the error of both methods (Fig. 5 and Table 5). For the lower terrace (Amuri Bluff terrace/Qt6), however, Ota et al.'s (1996) estimated age of 59 ± 3 ka is younger than our IRSL age of 74 ± 9 ka. Although not coinciding with the peak of any major sea-level high stand (Siddall et al., 2007), this age suggests deposition during the end of MIS 5a (Fig. 5).

The Kemps Hill terrace (Qt5), which lies between the Tarapuhi (Qt4) and Amuri Bluff (Qt6) terraces in elevation (Ota et al., 1984) must have formed sometime between the two. Most likely, it formed during the early part of MIS 5a because the Tarapuhi and Amuri Bluff terraces appear to be from the later parts of MIS 5c and 5a, respectively (Fig. 5), but a late 5c age cannot be ruled out.

For the low (4.2 m asl) Torlesse terrace northwest of Haumuri Bluff, both ^{14}C and AAR give Holocene ages (Fig. 5). Two of the three ^{14}C ages, HB4 (3.37–3.12 ka) and HB5-B (3.42–3.16 ka), agree, whereas HB5-D (6.99–5.41 ka) is outside the 2-sigma range of the other two (Table 3). Although the older age is closer to the AAR estimate, we rejected HB5-D because the ^{14}C laboratory reported analytical issues as described previously. The younger ^{14}C ages nonetheless overlap the 95% confidence intervals for the 6^{+16}_{-4} and 8^{+17}_{-5}ka age estimates for the two AAR samples (Table 5). The proportionately large uncertainty in the AAR age of Holocene shells likely reflects the difficulty in applying a calibration model based primarily on Pleistocene data, given the change in temperature and thus racemization rate at the close of the Pleistocene and, in this case, possible differences in racemization rate between *T. spissa* and *L. crassicosta*. Although we prefer the late Holocene ^{14}C ages over the middle Holocene AAR ages for the shells of the Torlesse terrace, we note that the marine unit that forms the Conway Flat surface, located 6 km to the southwest at 12 m asl also dates to the middle Holocene (7.0–8.6 ka; Ota et al., 1984). On the other hand, the AAR calibration curve seems to have overestimated the age of the Cape Kidnappers sample,

https://doi.org/10.1017/qua.2016.9 Published online by Cambridge University Press

which is likewise Holocene and not *T. spissa*, so the same effects may be responsible here.

Terrace correlations across the study areas

We have numbered the terraces in our three study areas as Qt1 to Qt8 from oldest to youngest (Table 1) using our geochronology to correlate terraces between localities. We correlate the Tiromoana terrace at Glenafric with the Tarapuhi terrace at Haumuri Bluff (both Qt4). Further, the Motunau terrace, which was previously thought to be the same age as or older than the Tiromoana terrace (Table 1), is now considered to be younger (Qt6) and is correlated with the Amuri Bluff terrace at the Haumuri Bluff locality.

The lack of an extensive MIS 5e terrace at all locations is surprising, considering the high stand was higher and lasted longer than subsequent high stands (Lambeck and Chappell, 2001; Siddall et al., 2007; Dutton and Lambeck, 2012) and that 5e marine terraces are common globally (Pedoja et al., 2014) and in other parts of New Zealand (Pillans, 1990). Nor do we find terraces of the same age at all three sites, with our best age estimates indicating MIS 5c terraces at Glenafric and Haumuri Bluff, MIS 5a terraces at Motunau Beach and Haumuri Bluff, and MIS 3 terrace reoccupation only at Motunau Beach. These observations can be explained by the destruction of older terraces by wave erosion during subsequent interstadial periods and by their dissection by fluvial processes during stadial periods. A stretch of cliffed coastline near Motunau Beach, for example, has retreated by 1.6 m/yr since 1950 (Barrell, 1989; Foster, 2009), although it was stable before that time, so the long-term average rate is likely less. As noted previously, small terrace remnants above the main terraces at Glenafric and Motunau Beach likely date from MIS 5e, based on their position relative to dated terraces (Fig. 5). That they are so poorly preserved compared with the MIS 5c or 5a terraces suggests that under the right conditions (presumably of rapid erosion and uplift), an MIS 5e terrace can be largely destroyed during these subsequent sea-level high stands. Differences in lithology, exposure to wave attack, and uplift rates among the three sites may explain the differences in terrace preservation at each location. This local variability, the lack of extensive MIS 5e terraces, and the unusual MIS 3 partial reoccupation of the seaward edge of one terrace all present a picture of a complex regime of terrace formation and preservation. Because of this complexity, terrace ages in North Canterbury, and anywhere else in which similar conditions may prevail, can be difficult to discern without the aid of numerical dating.

Although the inner edge of each terrace likely formed during the peak of the corresponding sea-level high stand, there is some evidence that the sediments and shells that we dated were deposited as sea level regressed. The most probable ages for IRSL samples HB2 and HB1 at Haumuri Bluff are from the young ends of MIS 5c and 5a, respectively (Fig. 5), although this is not certain within 95% confidence. In addition, at Motunau Beach, the preferred ages for samples MB6, MB5, MB4, and MB3 are progressively younger with distance away from the terrace inner edge (Table 5 and Fig. 3b), suggesting that they were deposited as the sea level retreated during MIS 5a (MB6 and MB5) and again during MIS 3 (MB4 and MB3), although the uncertainties in the AAR results are large enough that the opposite cannot be completely ruled out. These two lines of evidence suggest deposition during regression, but further investigation is needed to confirm or refute this hypothesis.

Comparison of dating techniques

AAR and IRSL are independent and complimentary techniques for dating Quaternary marine terraces. The range of factors that are incorporated into AAR age uncertainties, including intershell variability and calibration statistics, tend to yield larger errors compared with those that are included in IRSL age uncertainties, which focus on analytical precision rather than geologic uncertainties such as incomplete zeroing of the luminescence signal. In this study, the conservative 95% confidence intervals on the AAR calibration estimated by Bayesian averaging span more than one MIS substage. In practice, our results show good agreement between the most likely stage or substage estimates from AAR and those of IRSL, except in the older part of the Motunau Beach terrace where the IRSL sample had analytical issues. Despite the differences in modern temperature among the sample sites (Table 4), the fit of the model to the calibration data did not show a temperature effect (Fig. 6), and the primarily North Island–based model proved applicable to the North Canterbury data set. AAR is also useful for correlating terraces independently of the errors associated with numerical-age calibration, such as the correlation of the Qt4 terrace from Glenafric with that from Haumuri Bluff. When IRSL and AAR results converge, we have considerably more confidence in the terrace age than if only one method were used. In this study, the methods agreed for terrace Qt4 at Glenafric and Haumuri Bluff and Qt7 at Motunau Beach. When the two methods do not agree, such as at terrace Qt6 in the Motunau Beach area, and when there is reason to doubt one of the results, as with the radioisotope disequilibrium in sample MB1, then we have additional evidence by which to exclude that result.

This study includes the first application of the Bayesian method of Allen et al. (2013) to develop an AAR calibration curve for a Pleistocene data set. It is also the first AAR study in New Zealand to analyze the intracrystalline fraction of amino acids. For Asp D/L, which correlates most strongly with sample age in the calibration data set, the intershell variability based on the intracrystalline amino acids was consistently lower than for shells analyzed using conventional techniques and A/I in previous studies. Specifically, for the four stratigraphic units that were analyzed both in this study and by Bowen et al. (1998), the average coefficient of variation ($\bar{x}/\sigma$) was 4% for intracrystalline (bleached) Asp D/L versus 9% for unbleached A/I.

https://doi.org/10.1017/qua.2016.9 Published online by Cambridge University Press

CONCLUSIONS

Using infrared stimulated luminescence and AAR analyses, we have developed a new chronology for the marine terraces of North Canterbury, and we have developed an AAR age model for Asp racemization in *T. spissa* that is applicable over a range of latitudes within New Zealand. This work provides the geochronological context for subsequent neotectonic studies of the region, for which marine terraces serve as important markers of uplift rate. More specifically:

1. The method of Allen et al. (2013) proved successful in developing an AAR calibration curve for a mostly Pleistocene data set, using Bayesian model fitting and Bayesian averaging of different possible models.
2. IRSL and AAR work well together for dating Quaternary marine terraces. Estimated ages from the two methods agree sufficiently well in most cases for a reliable MIS assignment, and disagreement between them in one case helped to confirm the inaccuracy of a suspect IRSL result.
3. Numerical dating of terraces is necessary to establish reliable ages. Our results suggest that using elevation or degree of fluvial dissection to date and correlate terraces is insufficient in this region because terraces of different ages are preserved at different sites. Our terrace ages and correlations differ significantly from most previous work (Table 1), which was based on such methods. Where previous numerical dating did exist for Qt4 at Haumuri Bluff (Ota et al., 1996), however, our results agree with that previous work.
4. Our new geochronological results indicate that the Tiromoana terrace at Glenafric and the Tarapuhi terrace at Haumuri Bluff were both formed during MIS 5c. The Amuri Bluff terrace at Haumuri Bluff is assigned to MIS 5a. The Motunau coastal plain consists principally of an MIS 5a terrace, which is correlated with the Amuri Bluff terrace, but it has been partially reoccupied during MIS 3. This variety of ages for the widest, most continuous terrace at each site shows that terrace preservation is locally variable.
5. Unexpectedly, our results do not support an MIS 5e age for any of the terraces sampled, although this age is common for terraces worldwide. We attribute this to rapid erosion rates.

ACKNOWLEDGMENTS

This research was funded by Geological Society of America Graduate Research grants, American Association of Petroleum Geologists Grants-in-Aid, Sigma Xi Grants-in-Aid of Research, a Shell Geosciences Energy Research Facilitation Award, and the Penn State Deike grant and Scholten-Williams-Wright Scholarship in Field Geology. The Amino Acid Geochronology Laboratory is supported by National Science Foundation award EAR-1234413. We would like to thank Mark Quigley, Peter Almond, and Uwe Rieser for assistance in the field; Alan Beu for identifying the mollusks; Ningsheng Wang for advice on interpreting the IRSL results; Katherine Whitacre for analyzing the AAR samples; and the many North Canterbury landowners who kindly allowed us access to their land. We would also like to thank two anonymous reviewers, whose comments have helped us to improve this paper.

Supplementary Materials

To view supplementary material for this article, please visit https://doi.org/10.1017/qua.2016.9

REFERENCES

Aitken, M.J., Bowman, S.G.E., 1975. Thermoluminescent dating: assessment of alpha particle contribution. *Archaeometry* 17, 132–138.

Allen, A.P., Kosnik, M.A., Kaufman, D.S., 2013. Characterizing the dynamics of amino acid racemization using time-dependent reaction kinetics: a Bayesian approach to fitting age-calibration models. *Quaternary Geochronology* 18, 63–77.

Alloway, B.V., Pillans, B.J., Sandhu, A.S., Westgate, J.A., 1993. Revision of the marine chronology in the Wanganui Basin, New Zealand, based on the isothermal plateau fission-track dating of tephra horizons. *Sedimentary Geology* 82, 299–310.

Almond, P.C., Moar, N.T., Lian, O.B., 2001. Reinterpretation of the glacial chronology of South Westland, New Zealand. *New Zealand Journal of Geology and Geophysics* 44, 1–15.

Almond, P.C., Shanhun, F.L., Rieser, U., Shulmeister, J., 2007. An OSL, radiocarbon and tephra isochron-based chronology for Birdlings Flat loess at Ahuriri Quarry, Banks Peninsula, Canterbury, New Zealand. *Quaternary Geochronology* 2, 4–8.

Barrell, D.J.A., 1989. Geomorphic Evolution and Engineering Geological Studies at Coastal Motunau, North Canterbury. PhD dissertation, University of Canterbury, Christchurch, New Zealand.

Barrell, D.J.A., Townsend, D.B., 2012. General Distribution and Characteristics of Active Faults and Folds in the Hurunui District, North Canterbury. GNS Science Consultancy Report 2012/113. Environment Canterbury Regional Council, Christchurch, New Zealand.

Berger, G.W., Pillans, B.J., Tonkin, P.J., 2001. Luminescence chronology of loess-paleosol sequences from Canterbury, South Island, New Zealand. *New Zealand Journal of Geology and Geophysics* 44, 501–516.

Berryman, K., 1993. Distribution, age, and deformation of late Pleistocene marine terraces at Mahia Peninsula, Hikurangi subduction margin, New Zealand. *Tectonics* 12, 1365–1379.

Beu, A.G., Edwards, A.R., 1984. New Zealand Pleistocene and late Pliocene glacio-eustatic cycles. *Palaeogeography, Palaeoclimatology, Palaeoecology* 46, 119–142.

Bloom, A.L., Broecker, W.S., Chappell, J.M.A., Matthews, R.K., Mesolella, K.J., 1974. Quaternary sea level fluctuations on a tectonic coast: new $^{230}Th/^{234}U$ dates from the Huon Peninsula, New Guinea. *Quaternary Research* 4, 185–205.

Bowen, D.Q., Pillans, B., Sykes, G.A., Beu, A.G., Edwards, A.R., Kamp, P.J.J., Hull, A.G., 1998. Amino acid geochronology of Pleistocene marine sediments in the Wanganui Basin: a New Zealand framework for correlation and dating. *Journal of the Geological Society* 155, 439–446.

Bull, W.B., 1984. Correlation of flights of global marine terraces. In: Morisawa, M., Hack, J.T. (Eds.), Tectonic Geomorphology: Proceedings of the 15th Annual Binghamton Geomorphology Symposium, September 1984. Allen & Unwin, Boston, pp. 129–152.

Bush, S.L., Santos, G.M., Xu, X., Southon, J.R., Thiagarajan, N., Hines, S.K., Adkins, J.F., 2013. Simple, rapid, and cost effective: a screening method for ^{14}C analysis of small carbonate samples. *Radiocarbon* 55, 631–640.

Cabioch, G., Ayliffe, L.K., 2001. Raised coral terraces at Malakula, Vanuatu, southwest Pacific, indicate high sea level during marine isotope stage 3. *Quaternary Research* 56, 357–365.

Cann, J.H., Belperio, A.P., Gostin, V.A., Rice, R.L., 1993. Contemporary benthic foraminifera in Gulf St Vincent, South Australia, and a refined Late Pleistocene sea-level history. *Australian Journal of Earth Sciences* 40(2), 197–211.

Carr, M.J., 1970. The Stratigraphy and Chronology of the Hawera Series Marginal Marine Succession of the North Canterbury Coast. PhD dissertation, University of Canterbury, Christchurch, New Zealand.

Carter, R.M., Naish, T.R., 1998. A review of Wanganui Basin, New Zealand: global reference section for shallow marine, Plio–Pleistocene (2.5–0 Ma) cyclostratigraphy. *Sedimentary Geology* 122, 37–52.

Chappell, J., 1983. A revised sea-level record for the last 300,000 years on Papua New Guinea. *Search* 14, 99–101.

Chappell, J., 2002. Sea level changes forced ice breakouts in the Last Glacial cycle: new results from coral terraces. *Quaternary Science Reviews* 21, 1229–1240.

Chappell, J., Omura, A., Esat, T., McCulloch, M., Pandolfi, J., Ota, Y., Pillans, B., 1996. Reconciliation of late Quaternary sea levels derived from coral terraces at Huon Peninsula with deep sea oxygen isotope records. *Earth and Planetary Science Letters* 141, 227–236.

Chappell, J., Shackleton, N.J., 1986. Oxygen isotopes and sea-level. *Nature* 324, 137–140.

Clarke, M.L., Rendell, H.M., 1997. Stability of the IRSL spectra of alkali feldspars. *Physica Status Solidi (b)* 199, 597–604.

Doğan, U., Koçyiğit, A., Varol, B., Özer, İ., Molodkov, A., Zöhra, E., 2012. Reply to the comments by Erdem Bikaroğlu on "MIS 5a and MIS 3 relatively high sea-level stands on the Hatay-Samandağ Coast, Eastern Mediterranean, Turkey". *Quaternary International* 262, 84–87.

Dutton, A., Lambeck, K., 2012. Ice volume and sea level during the last interglacial. *Science* 337, 216–219.

Forsyth, P.J., Barrell, D.J.A., Jongens, R. (compilers) 2008. Geology of the Christchurch Area. Institute of Geological and Nuclear Sciences 1:250,000 Geological Map 16. GNS Science, Lower Hutt, New Zealand.

Foster, D., 2009. The Morphodynamics of Motunau Beach and Management Implications. Master's thesis, University of Canterbury, Christchurch, New Zealand.

Goodfriend, G.A., Kashgarian, M., Harasewych, M.G., 1995. Use of aspartic acid racemization and post-bomb ^{14}C to reconstruct growth rate and longevity of the deep-water slit shell *Entemnotrochus adansonianus*. *Geochimica et Cosmochimica Acta* 59, 1125–1129.

Guérin, G., Mercier, N., Adamiec, G., 2011. Dose-rate conversion factors: update. *Ancient TL* 29, 5–8.

Higham, T.F.G., Hogg, A.G., 1995. Radiocarbon dating of prehistoric shell from New Zealand and calculation of the ΔR values using fish otoliths. *Radiocarbon* 37, 409–416.

Hoeting, J.A., Madigan, D., Raftery, A.E., Volinsky, C.T., 1999. Bayesian model averaging: a tutorial. *Statistical Science* 14, 382–401.

Hormes, A., Preusser, F., Denton, G., Hajdas, I., Weiss, D., Stocker, T.F., Schlüchter, C., 2003. Radiocarbon and luminescence dating of overbank deposits in outwash sediments of the Last Glacial Maximum in North Westland, New Zealand. *New Zealand Journal of Geology and Geophysics* 46, 95–106.

Hull, A.G., 1987. A late Holocene marine terrace on the Kidnappers coast, North Island, New Zealand: some implications for shore platform development processes and uplift mechanism. *Quaternary Research* 28, 183–195.

Huntley, D.J., Lamothe, M., 2001. Ubiquity of anomalous fading in K-feldspars and the measurement and correction for it in optical dating. *Canadian Journal of Earth Sciences* 38, 1093–1106.

Huntley, D.J., Lian, O.B., 2006. Some observations on tunnelling of trapped electrons in feldspars and their implications for optical dating. *Quaternary Science Reviews* 25, 2503–2512.

Jobberns, G., 1926. Raised beaches in Teviotdale District, North Canterbury. *Transactions of the New Zealand Institute* 56, 225–226.

Jobberns, G., 1928. The raised beaches of the north east coast of the South Island of New Zealand. *Transactions of the New Zealand Institute* 59, 508–570.

Jobberns, G., King, L.C., 1933. The nature and mode of origin of the Motunau Plain, North Canterbury, New Zealand. *Transactions of the New Zealand Institute* 63, 355–369.

Kamp, P.J.J., Vonk, A.J., Bland, K.J., Hansen, R.J., Hendy, A.J.W., McIntyre, A.P., Ngatai, M., Cartwright, S.J., Hayton, S., Nelson, C.S., 2004. Neogene stratigraphic architecture and tectonic evolution of Wanganui, King County, and eastern Taranaki Basins, New Zealand. *New Zealand Journal of Geology and Geophysics* 47(4), 625–644.

Kaufman, D.S., Forman, S.L., Lea, P.D., Wobus, C.W., 1996. Age of pre-late-Wisconsin glacial-estuarine sedimentation, Bristol Bay, Alaska. *Quaternary Research* 45, 59–72.

Kaufman, D.S., Manley, W.F., 1998. A new procedure for determining DL amino acid ratios in fossils using reverse phase liquid chromatography. *Quaternary Science Reviews* 17, 987–1000.

Kelsey, H.M., Bockheim, J.G., 1994. Coastal landscape evolution as a function of eustasy and surface uplift rate, Cascadia margin, southern Oregon. *Geological Society of America Bulletin* 106, 840–854.

Kohn, B.P., Pillans, B., McGlone, M.S., 1992. Zircon fission track age for middle Pleistocene Rangitawa Tephra, New Zealand: stratigraphic and paleoclimatic significance. *Palaeogeography, Palaeoclimatology, Palaeoecology* 95, 73–94.

Krbetschek, M.R., Rieser, U., Stolz, W., 1996. Optical dating: some luminescence properties of natural feldspars. *Radiation Protection Dosimetry* 66, 407–412.

Lajoie, K.R., 1986. Coastal tectonics. In: Active Tectonics: Impact on Society. National Academy Press, Washington, D.C., pp. 95–124.

Lajoie, K.R., Wehmiller, J.F., Kennedy, G.L., 1980. Inter- and intrageneric trends in apparent racemization kinematics of amino acids in Quaternary mollusks. In: Hare, P.E., Hoering, T.C., King, K., (Eds.), Biogeochemistry of Amino Acids: Papers Presented at a Conference at Airlie House, Warrenton, Virginia, October 29 to November 1, 1978. Wiley, New York, pp. 305–340.

Lambeck, K., Chappell, J., 2001. Sea level change through the last glacial cycle. *Science* 292, 679–686.

Lisiecki, L.E., Raymo, M.E., 2005. A Pliocene-Pleistocene stack of 57 globally distributed benthic $\delta^{18}O$ records. *Paleoceanography* 20, PA1003. http://dx.doi.org/10.1029/2004PA001071.

Mallinson, D., Burdette, K., Mahan, S., Brook, G., 2008. Optically stimulated luminescence age controls on late Pleistocene and Holocene coastal lithosomes, North Carolina, USA. *Quaternary Research* 69, 97–109.

Manley, W.F., Miller, G.H., Czywczynski, J., 2000. Kinetics of aspartic acid racemization in *Mya* and *Hiatella*: modeling age and paleotemperature of high-latitude Quaternary mollusks. In: Goodfriend, G.A., Collins, M.J., Fogel, M.L., Macko, S.A., Wehmiller, J.F. (Eds.), *Perspectives in Amino Acid and Protein Geochemistry*. Oxford University Press, New York, pp. 202–218.

Mitterer, R.M., Kriausakul, N., 1989. Calculation of amino acid racemization ages based on apparent parabolic kinetics. *Quaternary Science Reviews* 8, 353–357.

Muhs, D.R., Rockwell, T.K., Kennedy, G.L., 1992. Late Quaternary uplift rates of marine terraces on the Pacific coast of North America, southern Oregon to Baja California Sur. *Quaternary International* 15–16, 121–133.

Murray, A.S., Wintle, A.G., 2000. Luminescence dating of quartz using an improved single-aliquot regenerative-dose protocol. *Radiation Measurements* 32, 57–73.

Murray-Wallace, C.V., Belperio, A.P., Gostin, V.A., Cann, J.H., 1993. Amino acid racemization and radiocarbon dating of interstadial marine strata (oxygen isotope stage 3), Gulf St. Vincent, South Australia. *Marine Geology* 110, 83–92.

Naish, T.R., Abbott, S.T., Alloway, B.V., Beu, A.G., Carter, R.M., Edwards, A.R., Journeaux, T.D., *et al*., 1998. Astronomical calibration of a Southern Hemisphere Plio-Pleistocene reference section, Wanganui Basin, New Zealand. *Quaternary Science Reviews* 17, 695–710.

Nicol, A., Alloway, B., Tonkin, P., 1994. Rates of deformation, uplift, and landscape development associated with active folding in the Waipara area of North Canterbury, New Zealand. *Tectonics* 13, 1327–1344.

Olley, J.M., Murray, A., Roberts, R.G., 1996. The effects of disequilibria in the uranium and thorium decay chains on burial dose rates in fluvial sediments. *Quaternary Science Reviews* 15, 751–760.

Ota, Y., Pillans, B., Berryman, K., Beu, A., Fujimori, T., Miyauchi, T., Berger, G., 1996. Pleistocene coastal terraces of Kaikoura Peninsula and the Marlborough coast, South Island, New Zealand. *New Zealand Journal of Geology and Geophysics* 39, 51–73.

Ota, Y., Yoshikawa, T., Iso, N., Okada, A., Yonekura, N., 1984. Marine terraces of the Conway coast, South Island, New Zealand. *New Zealand Journal of Geology and Geophysics* 27, 313–325.

Pedoja, K., Husson, L, Johnson, M.E., Melnick, D., Witt, C., Pochat, S., Nexer, M., *et al*., 2014. Coastal staircase sequences reflecting sea-level oscillations and tectonic uplift during the Quaternary and Neogene. *Earth-Science Reviews* 132, 13–38.

Penkman, K.E.H., Kaufman, D.S., Maddy, D., Collins, M.J., 2008. Closed-system behaviour of the intra-crystalline fraction of amino acids in mollusc shells. *Quaternary Geochronology* 3, 2–25.

Pettinga, J.R., Campbell, J.K., 2003. North Canterbury GIS. Unpublished maps, University of Canterbury, Christchurch, New Zealand.

Pettinga, J.R., Yetton, M.D., Van Dissen, R.J., Downes, G., 2001. Earthquake source identification and characterisation for the Canterbury region, South Island, New Zealand. *Bulletin of the New Zealand Society for Earthquake Engineering* 34, 282–317.

Pillans, B., 1983. Upper Quaternary marine terrace chronology and deformation, South Taranaki, New Zealand. *Geology* 11, 292–297.

Pillans, B., 1990. Pleistocene marine terraces in New Zealand: a review. *New Zealand Journal of Geology and Geophysics* 33, 219–231.

Pillans, B., Alloway, B., Naish, T., Westgate, J., Abbott, S., Palmer, A., 2005. Silicic tephras in Pleistocene shallow-marine sediments of Wanganui Basin, New Zealand. *Journal of the Royal Society of New Zealand* 35(1–2), 43–90.

Pillans, B., Holgate, G., McGlone, M., 1988. Climate and sea level during oxygen isotope stage 7b: on-land evidence from New Zealand. *Quaternary Research* 29, 176–185.

Powell, A.W.B., 1979. *New Zealand Mollusca: Marine, Land, and Freshwater Shells*. Collins, Auckland, New Zealand.

Prescott, J.R., Hutton, J.T., 1994. Cosmic ray contributions to dose rates for luminescence and ESR dating: large depths and long-term time variations. *Radiation Measurements* 23, 497–500.

Preusser, F., Andersen, B.G., Denton, G.H., Schlüchter, C., 2005. Luminescence chronology of Late Pleistocene glacial deposits in North Westland, New Zealand. *Quaternary Science Reviews* 24, 2207–2227.

Rattenbury, M.S., Townsend, D.B., Johnston, M.R. (compilers) 2006. Geology of the Kaikoura Area. Institute of Geological and Nuclear Sciences 1:250,000 Geological Map 13. GNS Science, Lower Hutt, New Zealand.

Reimer, P.J., Bard, E., Bayliss, A., Beck, J.W., Blackwell, P.G., Ramsey, C.B., Buck, C.E., *et al*., 2013. IntCal13 and Marine13 radiocarbon age calibration curves, 0-50,000 years cal BP. *Radiocarbon* 55, 1869–1887.

Rodriguez, A.B., Anderson, J.B., Banfield, L.A., Taviani, M., Abdulah, K., Snow, J.N., 2000. Identification of a –15 m middle Wisconsin shoreline on the Texas inner continental shelf. *Palaeogeography, Palaeoclimatology, Palaeoecology* 158, 25–43.

Rose, R.V., 2011. Quaternary Geology and Stratigraphy of North Westland, South Island, New Zealand. PhD dissertation, University of Canterbury, Christchurch, New Zealand.

Rother, H., Shulmeister, J., Rieser, U., 2010. Stratigraphy, optical dating chronology (IRSL) and depositional model of pre-LGM glacial deposits in the Hope Valley, New Zealand. *Quaternary Science Reviews* 29, 576–592.

Rowan, A.V., Roberts, H.M., Jones, M.A., Duller, G.A.T., Covey-Crump, S.J., 2012. Optically stimulated luminescence dating of glaciofluvial sediments on the Canterbury Plains, South Island, New Zealand. *Quaternary Geochronology* 8, 10–22.

Schwarz, G., 1978. Estimating the dimension of a model. *Annals of Statistics* 6, 461–464.

Shane, P.A.R., Black, T.M., Alloway, B.V., Westgate, J.A., 1996. Early to middle Pleistocene tephrochronology of North Island, New Zealand: Implications for volcanism, tectonism, and paleoenvironments. *GSA Bulletin* 108, 915–925.

Shulmeister, J., Thackray, G.D., Rieser, U., Hyatt, O.M., Rother, H., Smart, C.C., Evans, D.J.A., 2010. The stratigraphy, timing and climatic implications of glaciolacustrine deposits in the middle Rakaia Valley, South Island, New Zealand.

Siddall, M., Chappell, J., Potter, E.-K., 2007. Eustatic sea level during past interglacials. *Developments in Quaternary Sciences* 7, 75–92.

Siddall, M., Rohling, E.J., Thompson, W.G., Waelbroeck, C., 2008. Marine isotope stage 3 sea level fluctuations: Data synthesis and new outlook. Reviews of Geophysics 46, RG4003.

Singarayer, J.S., Bailey, R.M., Ward, S., Stokes, S., 2005. Assessing the completeness of optical resetting of quartz OSL in the natural environment. *Radiation Measurements* 40, 13–25.

Suggate, R.P., 1965. Late Pleistocene Geology of the Northern Part of the South Island, New Zealand. New Zealand Geological Survey Bulletin 77. Department of Scientific and Industrial Research, New Zealand Geological Survey, Wellington.

Trenhaile, A.S., 2002. Modeling the development of marine terraces on tectonically mobile rock coasts. *Marine Geology* 185, 341–361.

Wang, Z., Jones, B.G., Chen, T., Zhao, B., Zhan, Q., 2013. A raised OIS 3 sea level recorded in coastal sediments, southern Changjiang delta plain, China. *Quaternary Research* 79, 424–438.

Warren, G., 1995. Geology of the Parnassus Area, Scale 1:50,000. Institute of Geological and Nuclear Sciences Geological Map 18. Institute of Geological and Nuclear Sciences Limited, Lower Hutt, New Zealand.

Williams, P.W., McGlone, M., Neil, H., Zhao, J.-X., 2015. A review of New Zealand palaeoclimate from the Last Interglacial to the global Last Glacial Maximum. *Quaternary Science Reviews* 110, 92–106.

Wilson, D.D., 1963. Geology of Waipara Subdivision. New Zealand Geological Survey Bulletin, n.s., 64. Department of Scientific and Industrial Research, New Zealand Geological Survey, Wellington.

Wright, J.D., Sheridan, R.E., Miller, K.G., Uptegrove, J., Cramer, B.S., Browning, J.V., 2009. Late Pleistocene sea level on the New Jersey margin: implications to eustasy and deep-sea temperature. *Global and Planetary Change* 66, 93–99.

Yokoyama, Y., Esat, T.M., Lambeck, K., 2001. Last glacial sea-level change deduced from uplifted coral terraces of Huon Peninsula, Papua New Guinea. *Quaternary International* 83–85, 275–283.

Yousif, H.S., 1987. The Applications of Remote Sensing to Geomorphological Neotectonic Mapping in North Canterbury, New Zealand. PhD dissertation, University of Canterbury, Christchurch, New Zealand.

https://doi.org/10.1017/qua.2016.9 Published online by Cambridge University Press